Powder Technology 437 (2024) 119578

Contents lists available at ScienceDirect

Powder Technology

journal homepage: www.journals.elsevier.com/powder-technology

Determination of the size of representative volume element for gap-graded granular materials

Xiusong Shi [a], Zihao He [a], Jidong Zhao [b], Jiaying Liu [c,d,*]

[a] Key Lab of Ministry of Education for Geomechanics and Embankment Engineering, Hohai University, Nanjing, China
[b] Hong Kong University of Science and Technology, Clearwater Bay, Kowloon, Hong Kong
[c] Department of Civil Engineering, Hangzhou City University, Hangzhou, China
[d] Zhejiang Engineering Research Center of Intelligent Urban Infrastructure, Hangzhou, China

HIGHLIGHTS

- Over seven hundred simulations are performed on gap-graded granular soils.
- The Chi-square test is adopted to recommend the RVE sizes for each gradings.
- The proper RVE size decreases with particle size ratio and increases with coarse fraction.
- Empirical equations are proposed for the RVE sizes of gap-graded soils.

GRAPHICAL ABSTRACT

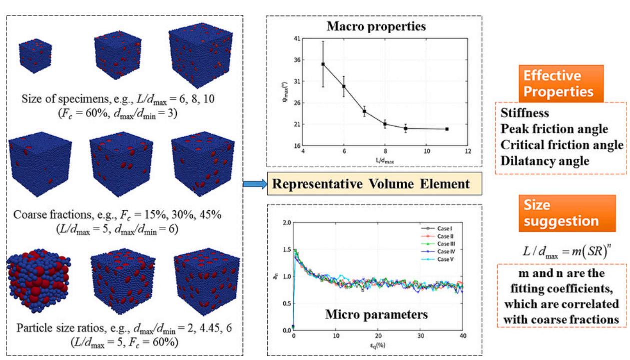

ARTICLE INFO

Keywords:
Gap-graded granular materials
DEM
Representative volume element
Particle size distribution
Size effect

ABSTRACT

Gap-graded granular soils have a wider grain size distribution and more heterogeneous fabric structure than normal soils. It is critical to choose the sample size of element tests in a faithful and repeatable manner. The Discrete Element Method (DEM) is utilized to determine the size of representative volume element (RVE) of gap-graded mixtures with varying particle size distributions. Over seven hundred triaxial tests are performed to investigate the effect of particle size ratio and coarse fraction on the typical RVE size. Microscopic parameters are analyzed to validate the reproducibility of the determined RVE sizes. The optimal RVE size is negatively proportional to particle size ratio and positively correlated with the coarse fraction. Empirical equations are further established to correlate the RVE sizes with particle size ratios for different coarse fractions. The findings may provide a useful reference for experimental and numerical studies in choosing the RVE size for gap-graded soils.

1. Introduction

The representative element volume is the minimum element volume at which the tested sample contains enough inhomogeneity to be statistically representative of the material under repeated testing [13,15,16,22,25,43,52]. Hudson and Harrison [25] introduced the RVE

* Corresponding author at: Department of Civil Engineering, Hangzhou City University, Hangzhou, China.
E-mail addresses: qingsongsaint@gmail.com (X. Shi), jzhao@ust.hk (J. Zhao), liujy@hzcu.edu.cn (J. Liu).

https://doi.org/10.1016/j.powtec.2024.119578
Received 20 December 2023; Received in revised form 2 February 2024; Accepted 26 February 2024
Available online 28 February 2024

concept and applied it in rock and soil mechanics for the measurement of macroscopic properties of the geological materials. Fig. 1 shows the conceptual diagram of RVE and scale-dependency of material properties. The mechanical properties of samples oscillate around an equilibrium magnitude, and the amplitude of the fluctuation decreases with increasing sample size and tends to vanish until the RVE size is reached. In multiscale modeling, the RVE is usually considered as a mesoscopic element to feed continuum modeling with the required material response and plays an important role in affecting the predictions of macroscopic behaviors of heterogeneous materials in different scales [16,20,56]. Hence, determining RVE size of granular materials is essential for faithfully predicting and understanding the effective properties of materials [11,24,37,44,56].

Numerous studies have been carried out, either in laboratory or using numerical approaches to investigate the RVE of heterogeneous materials in recent years (e.g., [7,11,13,18,30,34,40,47,57,59,67]). The consistency of the laboratory results may be questionable due to the change of structure and degradation of aggregates during the sample preparation. Moreover, the evolution of internal structure cannot be easily tracked during a loading process using conventional laboratory methods. To this end, numerical methods, including the finite element method (FEM) [14,16,61,67] and discrete element method (DEM) [10,11,30,56], become appealing in analyzing the RVE of granular soils. It has been reported that the RVE size may vary depending on different physical properties or material types [16,31,56]. For example, Gitman [16] investigated the RVE size of a three-phase heterogeneous material using FEM and found that the RVE size depends on the stress levels, corresponding to different loading regime of material response. Additionally, Wiacek and Molenda [56] observed that the RVE size of polydisperse granular material for porosity is larger than that for mechanical properties, such as elastic modulus and coordination number.

It has been recognized that the RVE size of granular material relies on the basic nature of granular particles, including the average grain size and grain size distribution. Schmidt et al. [46] showed that 5 to 6 times the mean grain diameter is required to reach an acceptable RVE size for Hostun sand in triaxial tests. Wiacek and Molenda [56] reported that 15 times the maximum grain size is required to minimize size effect of a sample with polydisperse granular packing in DEM simulations. The work after Ng and Zhou [37] on size effect of binary mixtures has shown that at least ten thousand particles are needed for consideration in a sample to obtain a RVE size, which is consistent with the recommended particle number in 2D DEM simulation conducted by Kuhn and Bagi [31].

Although the RVE of granular soils have been well documented in numerical studies, it remains debatable on the determination of RVE size due to the complex nature of particles. The suggested RVE size based on numerical analysis is not well consistent with standards or experimental studies. According to the American Society for Testing and Materials (ASTM) (2011) standard, the diameter of a sample should be at least 6 times the largest particle size in triaxial tests regardless of the gradings.

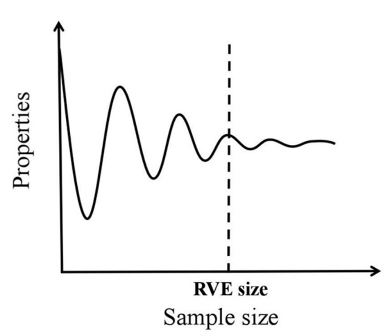

Fig. 1. Scale-dependency of soil properties and the concept of Representative Volume Element (RVE). Modified after Hudson and Harrison [25].

Al-Raoush and Papadopoulos [3] reported that the sample diameter should not be <4 times the maximum grain size for a sub-rounded sand. Furthermore, many geological process and industrial application involve granular materials featured with a discontinuous grading and a wide size distribution, resulting in an extreme internal heterogeneity [38,49,50,54,55,60,69,71,72]. However, most of the existing studies have been focused on the RVE size of narrow-graded soils [31,56]. It is well recognized that the grading significantly affects the effective properties of gap-graded soils, and therefore RVE size may vary with the gradings, e.g., particle size ratio and coarse fraction. However, there is no reported instruction in standards for gap-graded soils, e.g., ASTM [5] and British Standard (BS) [8]. Accordingly, there is a strong need for a systematical study on the size effect of sample size to provide a reference for selecting RVE size for future studies of gap-graded soils.

Indeed, how size effect of samples varies with coarse fraction and particle size ratio over their respective full ranges has not been fully understood for gap-graded soils. This paper offers a systematic study on the determination of RVE sizes for gap-graded soils with different gradings, highlighting the effect of coarse fraction and particle size ratio on the recommended RVE sizes. Triaxial compression tests of binary mixtures, polydisperse gap-graded mixtures and binary ellipsoid mixtures are studied by DEM, based on which Chi-square test is utilized to determine the RVE size. Microscopic information is extracted to verify the reproducibility of the selected RVE sizes. Empirical correlations are further established between RVE size and particle size ratio for various coarse fractions and are confirmed for different relative densities.

2. DEM simulation and methods

DEM simulations are conducted to investigate the RVE size of gap-graded granular materials. The binary mixtures are composed of two mono-sized components, coarse and fine spherical grains. The polydisperse gap-graded mixtures are prepared as supplementary samples which demonstrate the universality of RVE sizes obtained from binary mixtures in engineering applications. The RVE size of gap-graded mixtures is affected by many factors, including particle size ratio and coarse fraction [37]. It is well recognized that the RVE size may be different when considering various mechanical properties [1,56]. Therefore, identification criteria of a comprehensive consideration should be employed to ascertain a relatively accurate RVE size. The following presents a brief introduction of the methodologies on DEM modeling, assembly generation and the general principle in determining RVE size.

2.1. Discrete element method

In this study, the numerical DEM simulations are performed using the open-source software YADE [51]. The Hertz-Mindlin contact law in conjunction with Coulomb's friction is followed to model the interparticle contact [35,42] where the normal contact force (F_n) is calculated according to:

$$F_n = \frac{4}{3}E^*\sqrt{R^*}\delta_n^{\frac{3}{2}} \tag{1}$$

where δ_n is the relative normal displacement. E^* and R^* are the equivalent elastic modulus and the equivalent radius, respectively. They can be computed as follows:

$$\frac{1}{E^*} = \frac{1-\nu_1^2}{E_1} + \frac{1-\nu_2^2}{E_2} \tag{2}$$

$$\frac{1}{R^*} = \frac{1}{R_1} + \frac{1}{R_2} \tag{3}$$

where R_1 and R_2 are the radii of grains in contact. E_1, ν_1 and E_2, ν_2 are the elastic modulus and Poisson's ratio of two contacting particles. Additionally, the tangential contact force (F_t) is given by

$$F_t = 8G^* \sqrt{R^* \delta_n} \delta_t \quad (4)$$

where δ_t is the tangential displacement. G^* is the equivalent shear modulus which is given by

$$G^* = \frac{2-\nu_1}{G_1} + \frac{2-\nu_2}{G_2} \quad (5)$$

where G_1 and G_2 are the shear modulus of two grains, which can be calculated from the elastic modulus and Poisson's ratio of contacting particles.

The shear force cannot exceed a limiting value which is determined by the Coulomb's friction law

$$F_t \le \mu F_n \quad (6)$$

where μ is the interparticle friction coefficient according to $\tan(\phi)$, where ϕ is the friction angle.

2.2. Generation of binary DEM samples for simulation of gap-graded granular soils

Binary assemblies of spherical particles with different sample sizes are generated following the schematic example in Fig. 2 to simulate gap-graded granular soils. The particle size distributions are characterized by particle size ratio (*SR*) and coarse fraction (F_c). Referring to crystallography, a *SR* value of 4.45, which distinguishes the packing structure of binary mixtures, is considered as a threshold [69,72]. Theoretically, a fine grain exactly embeds in the pore bounded by four tangent large grains to form a typical packing structure when $SR = 4.45$, as shown in Fig. 3. For $SR < 4.45$, the coarse particles are separated by the fine particle; for $SR > 4.45$, the fine grain is too small to contact with the four coarse grains. Accordingly, five particle size ratios, i.e., $SR = d_{\max}/d_{\min} = 2$, 3, 4.45, 6, and 8 are selected for each coarse fraction, where the $d_{\max}$ and $d_{\min}$ are the diameters of coarse and fine particles, respectively. Six coarse fractions, i.e., $F_c = 15$, 30, 45, 60, 75 and 90% are considered. Furthermore, two extra particle size distributions, considering the polydispersity in both coarse and fine grain sizes, are supplemented for proving the general applicability of the RVE sizes of binary mixtures.

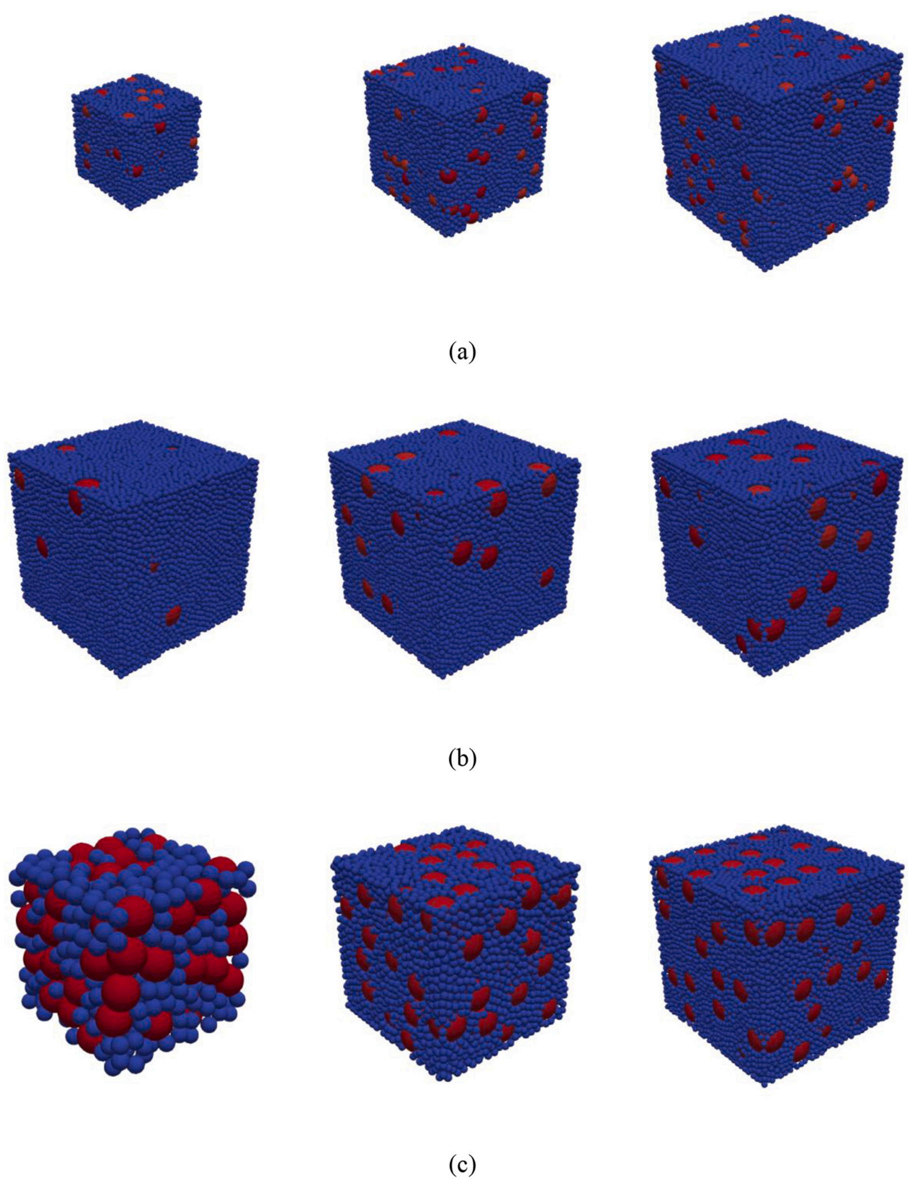

Fig. 2. The schematic view of numerical samples: (a) size of specimens, from left to right $L/d_{\max} = 6$, 8, 10 ($F_c = 60\%$, $d_{\max}/d_{\min} = 3$), (b) coarse fractions, from left to right $F_c = 15\%$, 30%, 45% ($L/d_{\max} = 5$, $d_{\max}/d_{\min} = 6$), (c) particle size ratios, from left to right $d_{\max}/d_{\min} = 2$, 4.45, 6 ($L/d_{\max} = 5$, $F_c = 60\%$).

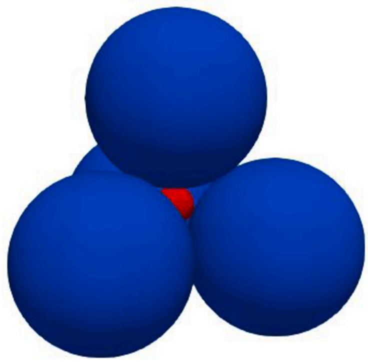

Fig. 3. The schematic view of the typical structure when SR = 4.45.

The effect of particle shape is investigated by binary mixtures of the prolate spheroids which have the same volumes with the spherical particles under the identical particle size distributions. The ratio of the major axis and minor axis is set as 1.5 for each ellipsoidal particle [29,37]. The gradings of the samples are presented in Fig. 4. Note that for the gradings in Fig. 4(a), the diameter of fine particle is set as a constant value 0.075 mm; for the gradings in Fig. 4(b), the diameter of coarse particle is 0.45 mm; for the gradings (PSD-1 and PSD-2) in Fig. 4 (c), the diameters of fine and coarse grains are continuously distributed in the ranges of [2/3 d_f, 4/3 d_f] and [2/3 d_c, 4/3 d_c], where d_f and d_c are the average diameters of fine and coarse grain, respectively [72]. A non-dimensional parameter ($L/d_{\max}$), termed as sample size ratio (SSR), is introduced herein to characterize the size effect. It is defined as the ratio of the initial length of cubic sample and the largest particle diameter. For each grading, the adopted range of sample size ratio can be different. The lower limit is 2, and the upper limit may vary on cases. Table 1 presents details of the SSRs for the simulation. More than seven hundred numerical tests are conducted to systematically investigate the RVE size of gap-graded granular materials.

Frictionless rigid walls are assumed to bound each generated sample. The study neglects gravity during the loading process. The Hertz-Mindlin contact model is adopted in the simulation [37]. The values of the material modulus, the Poisson's ratio, the particle density and the inter-grain friction angle are 30GPa, 0.15, 2600 kg/m^3 and 35°, respectively. The preparation process of the samples is divided into two stages: The maximum and minimum void ratio of gap-graded mixtures ($e_{\max}$, $e_{\min}$) will be acquired firstly to calculate the relative density, before samples with desired void ratios are generated for simulations. Three steps are followed to obtain the maximum and minimum void ratios:

1. A cloud of non-overlapping spheres with a diameter of approximately one half of the target size are generated within a cubic box bounded by frictionless walls;

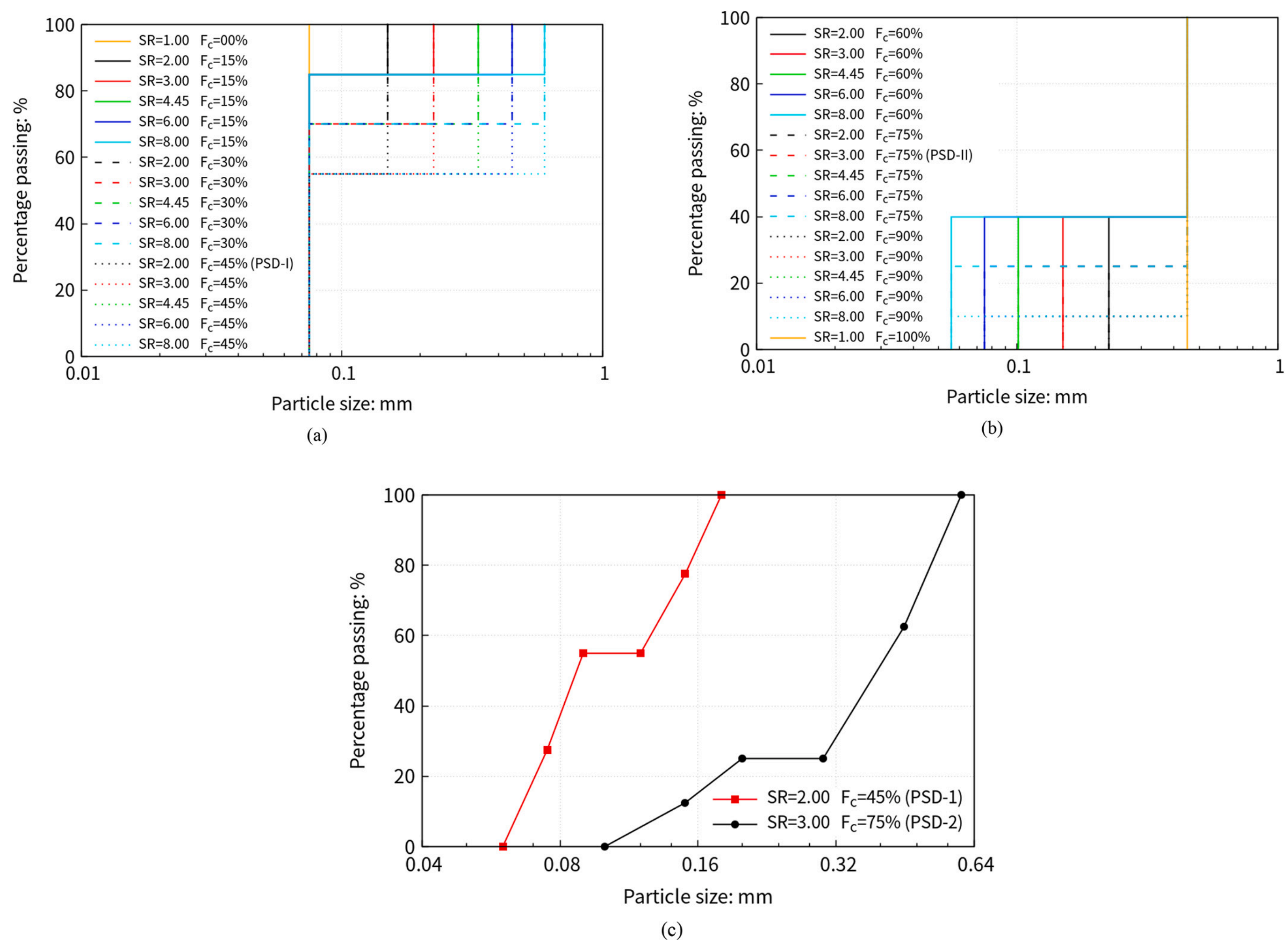

Fig. 4. Particle size distribution curves: (a) F_c = 00%, 15%, 30%, 45%, (b) F_c = 60%, 75%, 90%, 100% (c) PSD-1(red), PSD-2(black). In the following research, we will focus on 2 key PSDs: PSD-I (F_c = 45%, SR = 2 in (a)) and PSD-II (F_c = 75%, SR = 3 in (b)). (For interpretation of the references to colour in this figure legend, the reader is referred to the web version of this article.)

Table 1
PSDs and sample size ratios used for DEM analysis.

Coarse fraction	Particle size ratios	Sample size ratios
00%	1	5, 6, 7, 8, 9, 10, 11, 12, 13, 15
	2	5, 6, 7, 8
	3	5, 6, 7
15%	4.45	3, 4, 5
	6	3, 4, 5
	8	2, 3, 4
	2	5, 6, 7, 8, 10
	3	5, 6, 7
30%	4.45	4, 5, 6
	6	3, 4, 5
	8	2, 3, 4
	2	5, 6, 7, 8, 9, 11
	3	5, 6, 7, 8
45%	4.45	3, 4, 5, 7
	6	3, 4, 5, 6
	8	2, 3, 4, 5
	2	5, 6, 7, 8, 9, 10, 12
	3	5, 6, 7, 8
60%	4.45	5, 6, 7, 8
	6	4, 5, 6
	8	4, 5, 6
	2	5, 6, 7, 8, 9, 10, 11, 12, 15
	3	5, 6, 7, 8, 9, 10, 11, 13
75%	4.45	5, 6, 7, 8, 9, 11
	6	5, 6, 7, 8, 10
	8	5, 6, 7, 8
	2	5, 6, 7, 8, 9, 10, 11, 12, 13, 15
	3	5, 6, 7, 8, 9, 10, 11, 12, 15
90%	4.45	5, 6, 7, 8, 9, 10, 12
	6	5, 6, 7, 8, 9, 10, 12
	8	5, 6, 7, 8
100%	1	5, 6, 7, 8, 9, 10, 11, 12, 13, 15

2. The grains are gradually dilated toward the target size using the radius expansion method (the friction coefficient between particles is set to 0);
3. The inter-particle friction angle is set to 0° or 35°, respectively, to isotropically compress the samples to a predefined size and a confining stress of 200 kPa, to obtain the minimum and maximum void ratios [53].

To render the simulations comparable, samples are so prepared to reach the same initial relative density after consolidation. The relative densities (D_r) of samples are selected to be 80% and 50% for an initially dense packing:

$$D_r = \frac{e_{\max} - e}{e_{\max} - e_{\min}} \tag{7}$$

It should be noted that the inter-particle friction angle is calibrated through trial-and-error method during the isotropic consolidation stage until the target void ratio is achieved. A relaxation stage is subsequently performed to ensure that the normalized unbalanced force ratio is lower than 0.01 for each simulation [36]. Finally, a friction angle of 35° is assigned to all particles, and the samples are sheared under a constant confining stress (200 kPa).

2.3. Determination of RVE size

Several methods have been previously proposed to determine the RVE size of granular materials [16,28,39,46,56], among which the combined numerical-statistical method is adopted in this study. For a given grading and sample size ratio, five realizations of samples with the identical size are generated to compute the statistic parameters of mechanical properties. Note that each realization may result in different internal microstructure, and each consolidated sample is then sheared to the critical state. A certain accuracy is prescribed to objectively find a RVE size on which the macroscopic mechanical properties are examined. Three mechanical parameters, namely, peak friction angle (ϕ_p), maximum dilatancy angle ($\psi_{\max}$), and critical state friction angle (ϕ_{cs}), are calculated from the obtained stress-strain and volumetric strain curves for determination of RVE size [1,31]:

$$\phi = arcsin\frac{\sigma_1 - \sigma_3}{\sigma_1 + \sigma_3} \tag{8}$$

$$\psi = arcsin\frac{d\varepsilon_v}{-2d\varepsilon_1 + d\varepsilon_v} \tag{9}$$

where σ_1 and σ_3 are the maximum and minimum principal stress, respectively; dε_v and dε_1 are the increments of volumetric strain and major principal strain, respectively.

Based on the simulated data of five realizations for each case, the average value, standard deviation, coefficient of variation and Chi-square value of the three mechanical parameters are adopted as indicators for evaluating the RVE size, which are expressed as

$$\overline{X} = \frac{1}{5}\sum_{n=1}^{n=5} X_n \tag{10}$$

$$X_{SD} = \sqrt{\frac{1}{5}\sum_{n=1}^{n=5}(X_n - \overline{X})^2} \tag{11}$$

$$COV = \frac{X_{SD}}{\overline{X}} \tag{12}$$

and

$$\chi^2 = \sum_{n=1}^{n=5}\frac{(X_n - \overline{X})^2}{\overline{X}} \tag{13}$$

where X_n is the value of mechanical property for the nth realization. $\overline{X}$, X_{SD}, COV and $\chi^2$are the mean value, standard deviation, coefficient of variation and Chi-square of five realizations for a certain sample size ratio, respectively.

Chi-square test has been widely accepted as a reliable method for determining the RVE size for different heterogeneous materials [16,26,46,62]. According to the Chi-square test in statistics, a critical Chi-square value of 0.103 is identified according to the distribution table by calculating the degree of freedom equal to 2 and setting a prescribed accuracy of 95%, which is mostly adopted for investigating the RVE size of granular materials in previous literatures [16,46]. Then, the χ^2 values of three mechanical parameters are calculated by Eq. (13) and compared with the table value. If the three Chi-square values are lower than the critical value, the corresponding sample size ratio satisfies the given accuracy and can be determined as RVE size [16]. For more details of Chi-square test, refer to the Appendix A.

3. Simulation results and analysis

The RVE size of gap-graded granular mixtures is related to particle size distribution (PSD) which can be featured by coarse fraction and particle size ratio. In the sequel, the sample size effect on the mechanical properties will be presented and the RVE size is determined based on the test results and the Chi-square criterion.

3.1. Determination of RVE size based on macroscopic properties

In this section, the simulation results are analyzed to determine the RVE size for each grading according to the Chi-square test. The following

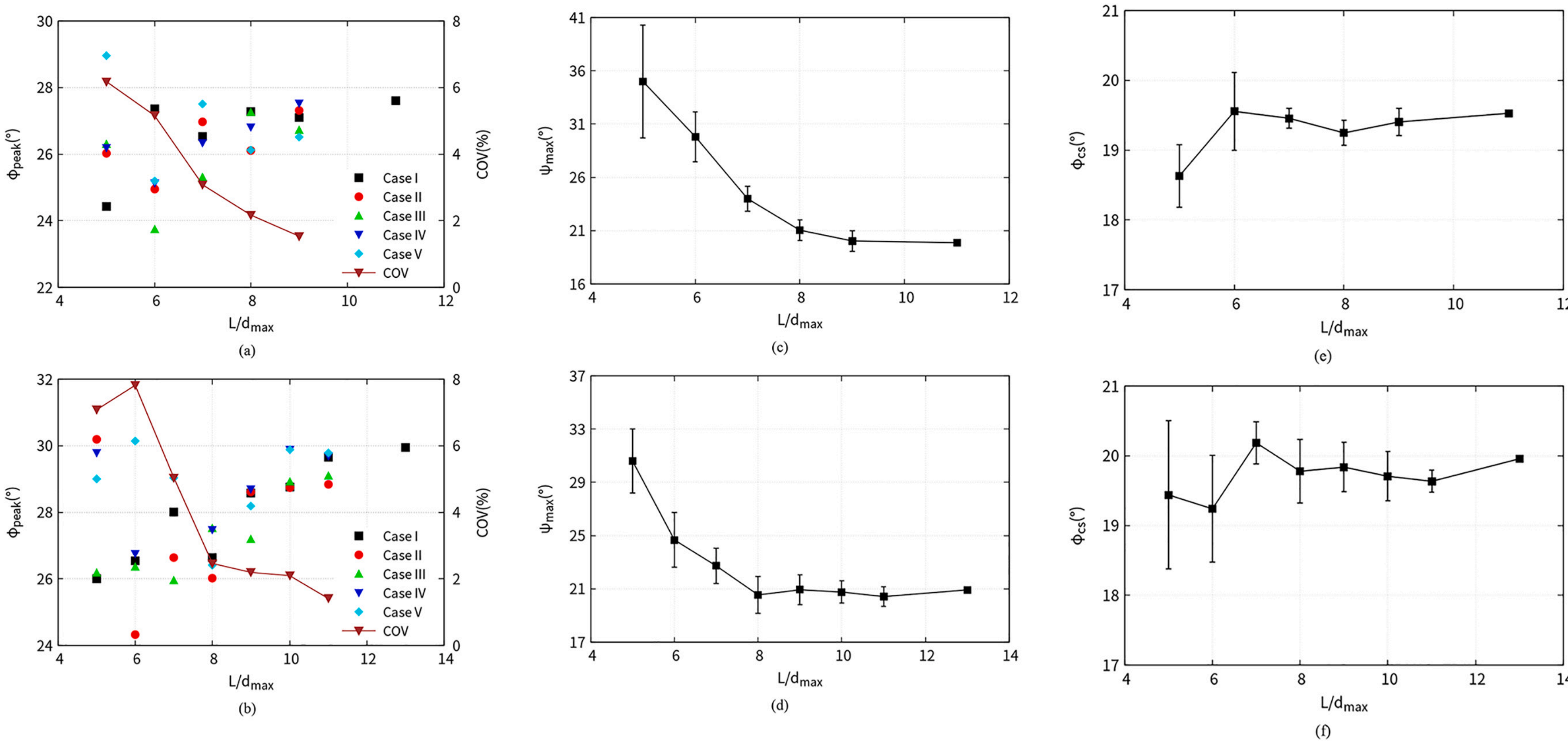

Fig. 5. Results of simulated macroscopic properties: (a)-(b) peak friction angle for PSD-I and PSD-II, (c)-(d) average value and standard deviation of maximum dilatancy angle for PSD-I and PSD-II, (e)-(f) average value and standard deviation of critical state friction angle for PSD-I and PSD-II.

analysis takes two particle size distributions $F_c = 45\%$, $SR = 2$ (PSD-I) in Fig. 4(a) and $F_c = 75\%$, $SR = 3$ (PSD-II) in Fig. 4(b) as examples.

Fig. 5 presents the evolutions of the three mechanical parameters calculated from the results of PSD-I and PSD-II. The change of strength properties with sample size ratios is shown in Fig. 5(a) and (b). For these two PSDs, the scatter of peak friction angles reduces with increasing sample size, which can be quantified by the COV. When the sample size ratios reach 9 and 11, the COVs of peak friction angles drop below 2%, indicating a convergence of this strength property. Fig. 5(c) and (d) present the standard deviation and average value of the maximum dilatancy angle of two gradings. Notably, both standard deviation and average value fall significantly with increasing sample size ratio and become stable when the sample size ratio reaches a certain threshold. In the case of PSD-I, the standard deviation falls below 1° when the sample size ratio increases to 8, and the mean value remains relatively constant until the sample size ratio exceeds 9. As for PSD-II, the average value starts to converge to a value of 21° when the sample size ratio approaches 8. The variation of critical state friction angle is illustrated in Fig. 5(e) and (f). The standard deviation shows a similar trend to that of the maximum dilatancy angle. The average value of this property shows a negligible change with a range of approximately 1°.

The RVE size is determined using the Chi-square test. The Chi-square values of three macroscopic properties of the two PSDs are calculated and plotted in Fig. 6. It is seen that the Chi-square values decrease with increasing sample size. For PSD-I, when the sample size ratio increases to 9, the Chi-square values of three mechanical properties are less than the critical value 0.103 (dashed line), satisfying the criterion. Analogously, a sample size ratio of 11 is required to approach the desired accuracy of 95% under repeated tests for PSD-II. Therefore, the RVE sizes of the two gradings are determined as 9 and 11, respectively.

The data of the supplemental tests on polydisperse gap-graded mixtures (PSD-1 and PSD-2) and binary ellipsoid mixtures (PSD-I and PSD-II) are also analyzed and examined using the same method, which is in agreement with those of binary mixtures (e.g. PSD-I and PSD-II). The similar results, listed in Appendix B, further demonstrate the applicability of the RVE sizes for the real gap-graded soils. Consequently, for the granular material with a wide particle size distribution in practice, once the coarse fraction and the ratio of representative diameters of fine and coarse particle are determined, the corresponding RVE size may be identified by referring to this work.

3.2. Verification of RVE size based on microscopic properties

The RVE bridges the microstructural heterogeneity and macro-mechanical properties of materials in multiscale analysis [16,20,21,23,41]. The macroscopic mechanical parameters are used to determine the RVE sizes in the previous section in order to assure that the RVE can be representative of the overall behaviors of particle assemblies. Furthermore, the evolution of microscopic statistical parameters is monitored to confirm that the RVE contains enough inhomogeneity. Herein, three quantities, including the coordination number, contact normal anisotropy (a_c) and normal force anisotropy (a_n), are extracted to verify the reproducibility of the RVE sizes of PSD-I and PSD-II [1,46,56]. The microscopic responses of both PSDs show a similar manner, thus the following analysis and comparison focus on PSD-I.

3.2.1. Coordination number

The coordination number is an indicative parameter for describing the evolving internal structure of a granular assembly, which is defined as the number of contacts for a given particle in a sample [45]. The average coordination number is analyzed herein to validate the RVE size. As illustrated in Fig. 7(a) and (b), the evolutions of the mean coordination number for samples of $L/d_{\max} = 6$ and $L/d_{\max} = 9$ in PSD-I are monitored in compressing process. For both cases, the coordination number shows a sharp drop initially, and then reaches a plateau until the axial strain increases to 10%. The exponential decay at the initial loading stage mainly originates from the spatial rearrangement of particles, which indicates the rapid loss of inter-particle contacts. In this process, some contact forces significantly grow to form strong force sub-networks to resist the increasing applied loading. Once the coordination numbers approach a relatively steady value, the contact network also reaches a balance state in which the rate of contact loss is dynamically equivalent to the rate of contact formation.

As shown in Fig. 7(a), it can be observed that the curves of the sample with lower sample size ratio are more fluctuant, clearly showing a poor reproducibility. However, the responses of five realizations for the larger sample nearly overlap in Fig. 7(b), which indicates that this sample size ratio serves as a better candidate for the RVE size. Similarly, referring to Fig. 7(c) and (d), it is feasible to determine $L/d_{max} = 11$ as the RVE size of PSD-II to ensure consistency of microscopic properties under repeated tests. The evolution of coordination number partly reveals the microscopic origin of the size effect. For the sample size below the RVE size, the oscillation of the coordination number denotes the rearrangements of grains without forming a stable contact network, which significantly affects the force transmission in the system. Consequently, the instability of the structure may lead to the variable macroscopic mechanical parameters. In contrast, the samples with the RVE size, possessing a robust skeleton to bear the load, may accurately predict the effective properties of the material.

3.2.2. Evolution of anisotropy

The evolution of anisotropy, including geometrical anisotropy and mechanical anisotropy, contributes to macroscopic characteristics during the loading process [6,19,63–66,68,70]. Two anisotropy invariants, the contact normal anisotropy and normal force anisotropy are monitored. As shown in Fig. 8, the evolution of a_c of all samples shows a softening trend with increasing axial strain, which is consistent with the literature [19,65]. The value of a_c rapidly rises within axial strain of 1%, then gradually increases to a peak at axial strain of 4% and decreases to the critical state. For the normal force anisotropy, the value of a_n in Fig. 9 presents a more significant softening trend compared to a_c. It sharply increases to a peak within a small strain level of 0.5%, then steadily decreases to a critical value at axial strain of around 15%.

The results presented in Figs. 8 and 9 highlight the reproducibility of the determined RVE sizes. As shown in Fig. 8(a) and (b), the curves of a_c of samples with $L/d_{\max} = 6$ oscillate drastically, but a_c of samples with the determined RVE size evolves smoothly, showing clearly a better reproducibility. Regarding to the normal force anisotropy, nonnegligible gaps and fluctuations can be observed between the curves of five realizations for the smaller samples in Fig. 9(a). By contrast, the a_n of the five RVE samples shows a replicable evolution as shown in Fig. 9(b). The responses of both anisotropy coefficients indicate that $L/d_{\max} = 9$ can be regarded as a desirable RVE size corresponding to PSD-I. Analogous conclusions can be obtained by comparing the anisotropy of samples of PSD-II to demonstrate that $L/d_{\max} = 11$ is a reliable RVE size. For the fluctuation of the anisotropy in small-scale samples, it may be explained by the slip-stick motion for the frictional contact [2,12,19]. The grains contained in the small-scale samples are too few to form a stable structure in which the inter-particle contacts are not robust and a mass of inter-particle sliding constantly occur throughout the loading process. Correspondingly, both the anisotropic responses and strength properties are variable and unrepresentative. Conversely, the samples with RVE size contain enough inhomogeneity and possess a strong contact network by which the applied loading is steadily transmitted from boundary to boundary. Thus, both the macroscopic and microscopic properties are reliable and reproducible.

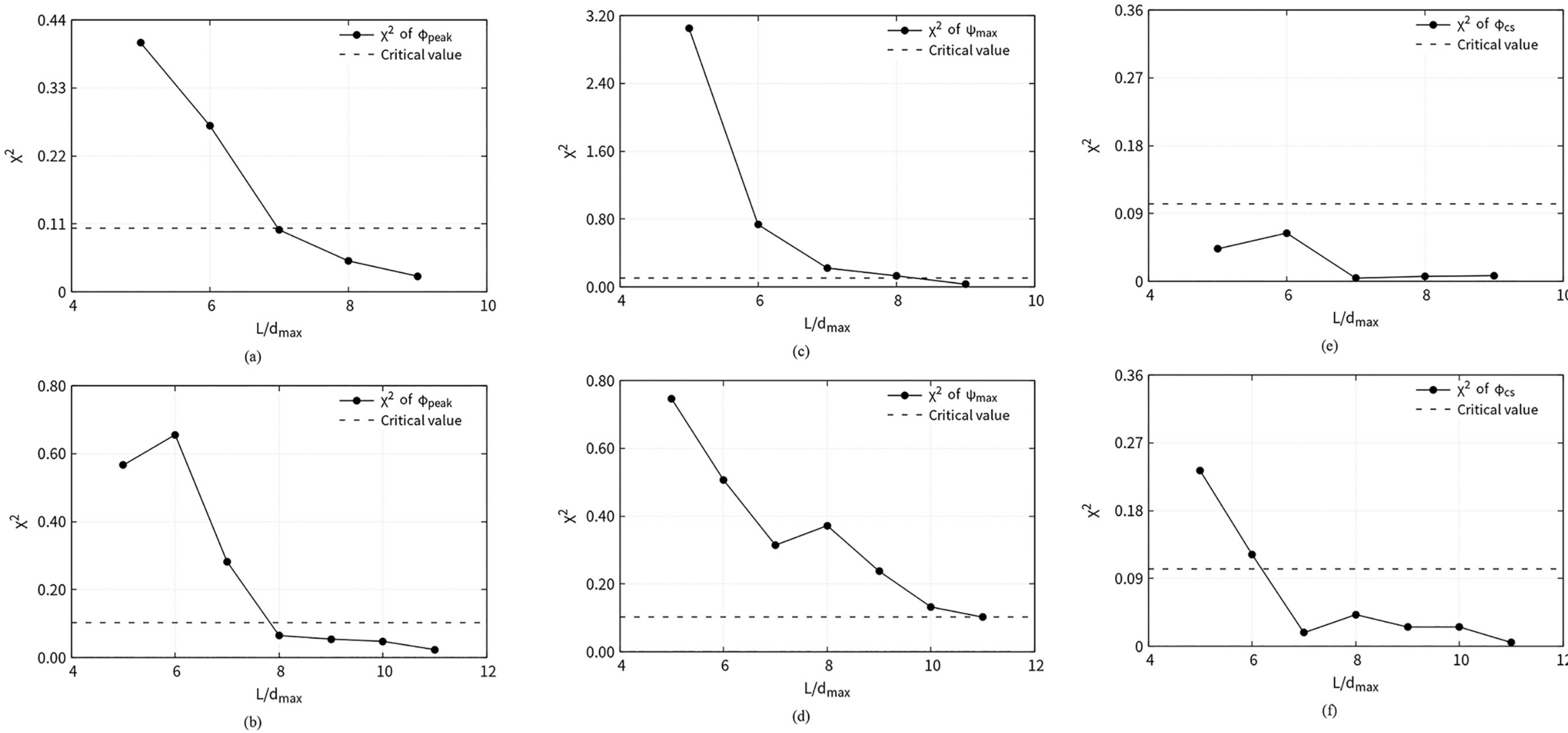

Fig. 6. Chi-square values of macroscopic properties: (a)-(b) Chi-square values of peak friction angle for PSD-I and PSD-II, (c)-(d) Chi-square values of maximum dilatancy angle for PSD-I and PSD-II, (e)-(f) Chi-square values of critical state friction angle for PSD-I and PSD-II.

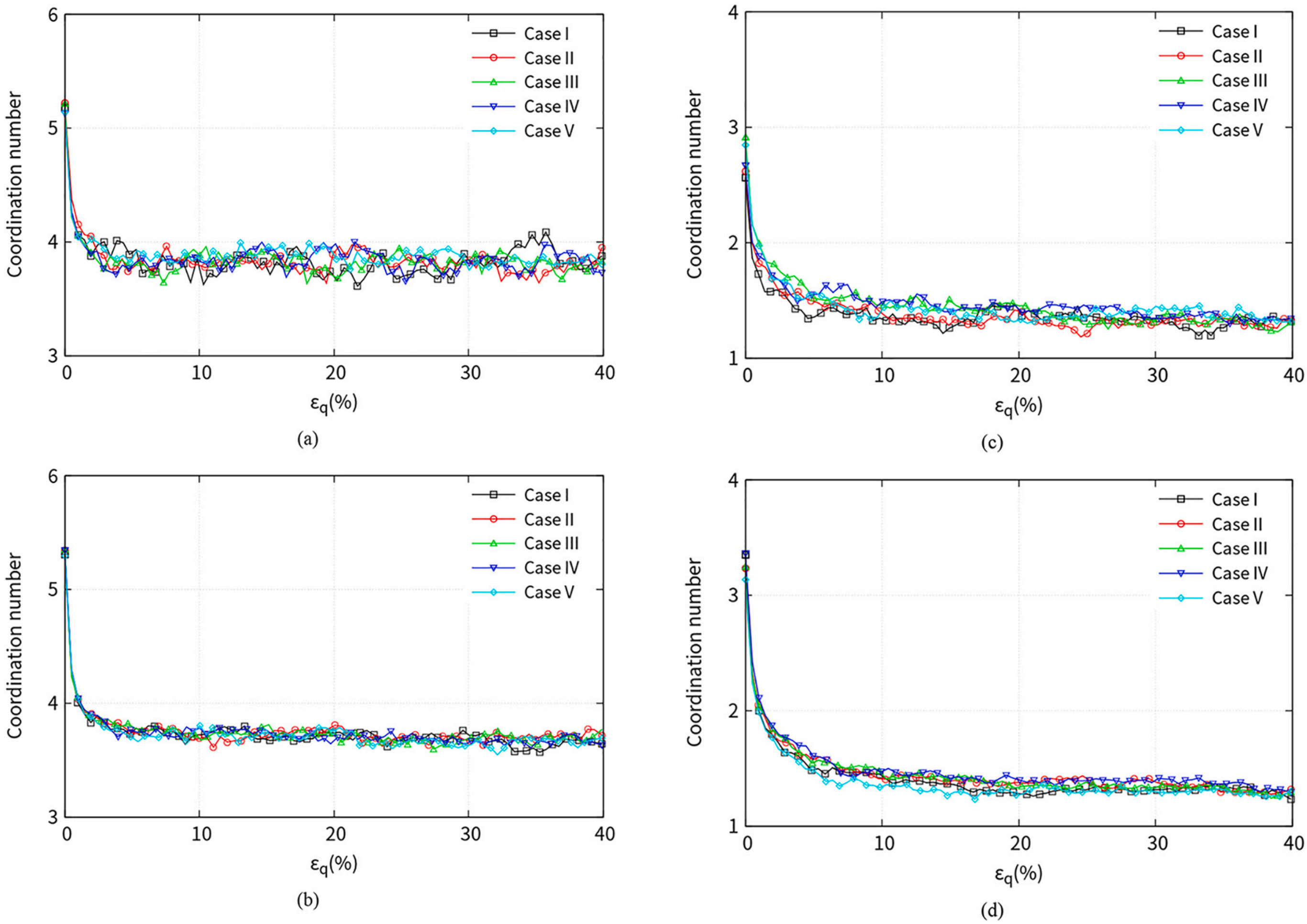

Fig. 7. Reproducibility of the average coordination number: (a) $L/d_{\max} = 6$ of PSD-I, (b) $L/d_{\max} = 9$ of PSD-I, (c) $L/d_{\max} = 8$ of PSD-II, (d) $L/d_{\max} = 11$ of PSD-II.

3.3. Effect of SR and F_cF$_c$ on the RVE size

As mentioned above, the RVE size relies on gradings of gap-graded granular mixtures. The influence of particle size ratio and coarse fraction are hereby investigated. Table 2 summarizes the values of RVE size for each particle size distribution, which may provide a reference for determining sample sizes both in lab and numerical triaxial tests. Fig. 10 illustrates the change of RVE sizes with particle size ratio in double logarithmic coordinates. Note that the purple symbols represent the RVE sizes of two uniform gradings, which are equal to 13 and distinct from those of gap gradings. It is evident that the RVE size decreases with rising particle size ratio but increases with growing coarse fraction. The solid lines are the fitting lines of RVE sizes of various gradings, which move upwards when coarse fraction increases and are characterized by the following expression:

$$L/d_{\max} = m(SR)^n \tag{14}$$

where m and n are the fitting coefficients, which are correlated with coarse fractions. The values of m and n are listed in Table 3. Their relationships with coarse fractions can be expressed by linear functions which are presented in Table 4 and plotted in Fig. 11. It shows that the two parameters increase with rising coarse fraction. Note that the average grain diameter (d_{50}) and uniformity coefficient (C_u) may also be used to establish relationships with the sample size ratio, but they depend on the coarse fraction and particle size ratio whose effects cannot be well distinguished. Therefore, the particle size ratio is adopted herein for the correlation with the RVE size, and the fitting coefficients have a further correlation with the coarse fraction.

Particularly, Eq. (14) is a power function obtained by establishing the empirical relationship between the RVE sizes and particles size ratios for the same relative density of 80%, which may need further confirmation for other relative density. To this end, another relative density of 50% is adopted for coarse fractions of 45% and 75% herein to demonstrate the applicability of Eq. (14). As shown in Fig. 12, the RVE sizes increase slightly compared to those for $D_r = 80\%$ due to the relatively loose internal structure, but the evolution of RVE sizes with particle size ratios still follows the power function as the Eq. (14) when the relative density is 50%. Hence, it could be assumed that the proposed empirical equation may reflect the relationship between RVE sizes and particle size ratios for various relative densities.

The effect of particle size ratio and coarse fraction on RVE size may be interpreted by heterogeneity of the internal structure of gap-graded soils. In Fig. 10, it could be noted that there is a gap between the fitting lines of $F_c = 75\%$ and 60%. The lower and upper sides of the gap are two dominant structure regions. For the region below the gap, the grains in RVE samples are compacted tightly to form a robust force network, in which fine and coarse particles play a dominant and strengthening role, respectively. For the region above the gap, the microstructure of samples becomes more heterogeneous as the particle size ratio and coarse fraction rise. An increasing proportion of loading is sustained by the coarse grain skeleton, and most of fine particles located in the voids are inactive or wedged between coarse grains in the coarse-

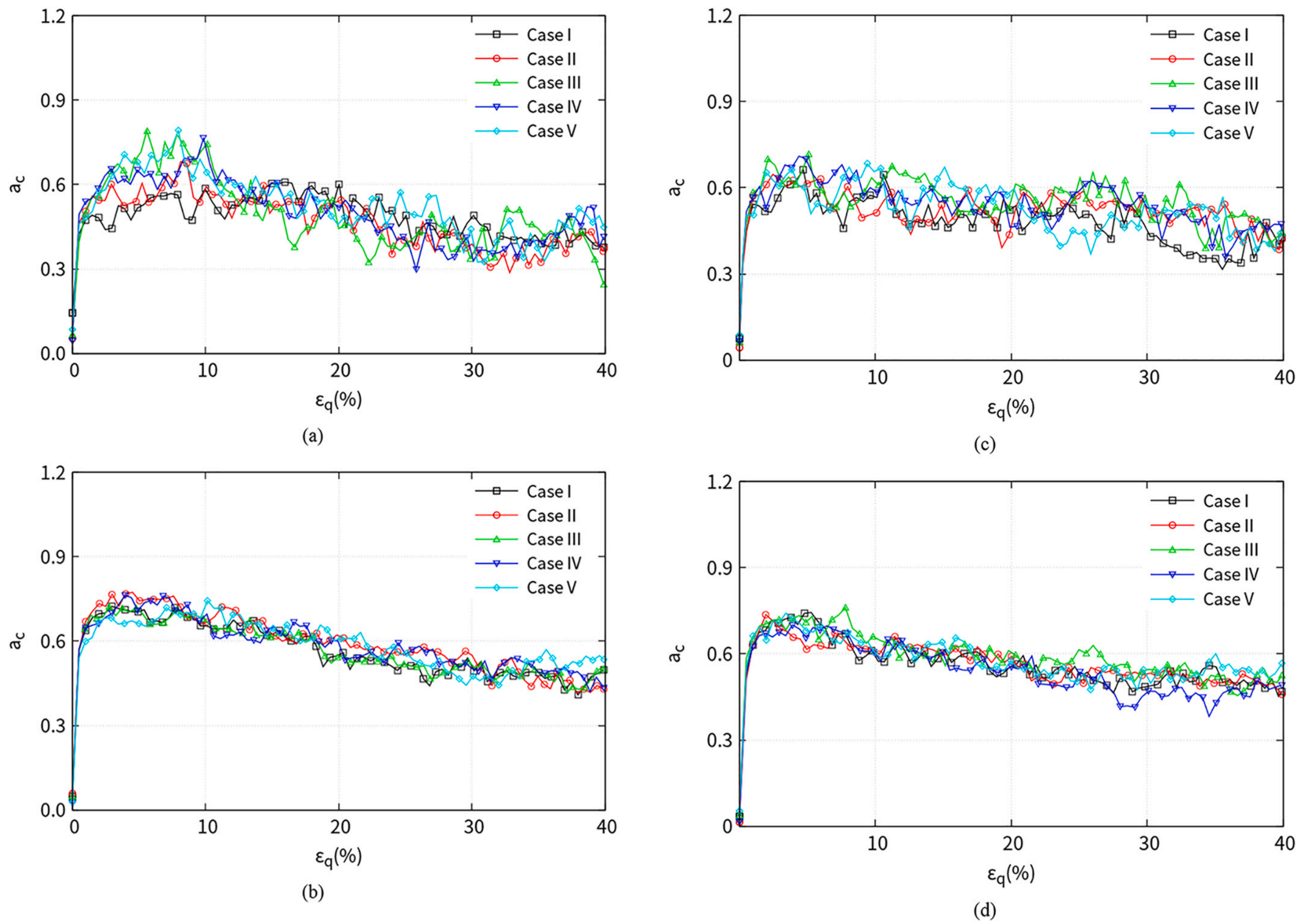

Fig. 8. Reproducibility of the contact normal anisotropy: (a) $L/d_{max} = 6$ of PSD-I, (b) $L/d_{max} = 9$ of PSD-I, (c) $L/d_{max} = 8$ of PSD-II, (d) $L/d_{max} = 11$ of PSD-II.

particle-dominant structure, which may lead to a loose and unstable force network [17,32,49]. Therefore, a higher sample size is suggested to ensure an adequate heterogeneity as well as a more reliable mechanical response for high coarse fraction. Unlike the dominant structure, the gap represents a transitional region originated from the threshold coarse fraction. The transitional coarse or fine fraction has been extensively investigated by laboratory tests and numerical simulation [58,60,68,71,73]. Herein, the initial void ratios of RVE samples are plotted in Fig. 13 to characterize the transitional coarse fraction. It could be observed that the transition zone is within the range of 60% to 75% for various particle size ratios, which exactly corresponds to the gap zone in Fig. 10. Consequently, it is reasonable to infer that the change of coarse fraction in the transition zone may affect the sensitive internal structure of the gap-graded mixtures, which further results in the noticeable separation between $F_c = 60\%$ and 75%. For the transition region, the effect of microstructure evolution on RVE size deserves further investigation in future research.

4. Discussion

4.1. Recommended sample sizes in standards

For a reliable macro-response in triaxial compression tests, ASTM (2011) standard recommends that the sample size should be at least 6 times the maximum particle size and no smaller than 33 mm. Similarly, BS standard (1990) suggests that the sample diameter should be at least 5 times the maximum grain size for triaxial element tests. However, these recommended sample sizes may not fully eliminate the size effect for gap-graded soils with a wide size distribution. In this work, the RVE sizes of gap-graded mixtures with various gradings are determined and their applicability for polydisperse gap-graded soils is also demonstrated. The empirical formulas are established to correlate RVE sizes and particle size ratios. Consequently, for a given gap-graded soil in the field, the coarse fraction and ratio of representative sizes of fine grains and coarse aggregates are readily available. Its RVE size can then be obtained by referring to Table 2 or Eq. (14). This study fills the gap for existing standards and provides a reference for determining sample size of gap-graded soils in element tests.

4.2. Mechanism of size effect

As illustrated in Fig. 5, the mechanical properties of gap-graded mixtures exhibit a notable scale-dependency. As the sample size ratio increases, the properties tend to converge, indicating a diminishing size effect. The trend may be attributed to the change of the microstructure which greatly depends on the nature of granular particles. The effect of grain size distribution has been studied by simplified binary mixtures in this work. The wider PSD leads to the larger RVE size, which results from the increasing heterogeneity of the particle size [3,4,9]. Furthermore, extra simulation tests, considering the effects of particle shape and polydispersity of gap-graded mixtures, show analogous trends with those of binary mixtures, which proves the feasibility of the determined RVE sizes. Nevertheless, the particles with realistic morphology would form a relatively more complex packing structure with more heterogeneity, which may complicate the mechanism of the size effect of gap-graded soils. This issue still requires further investigation to clarify the

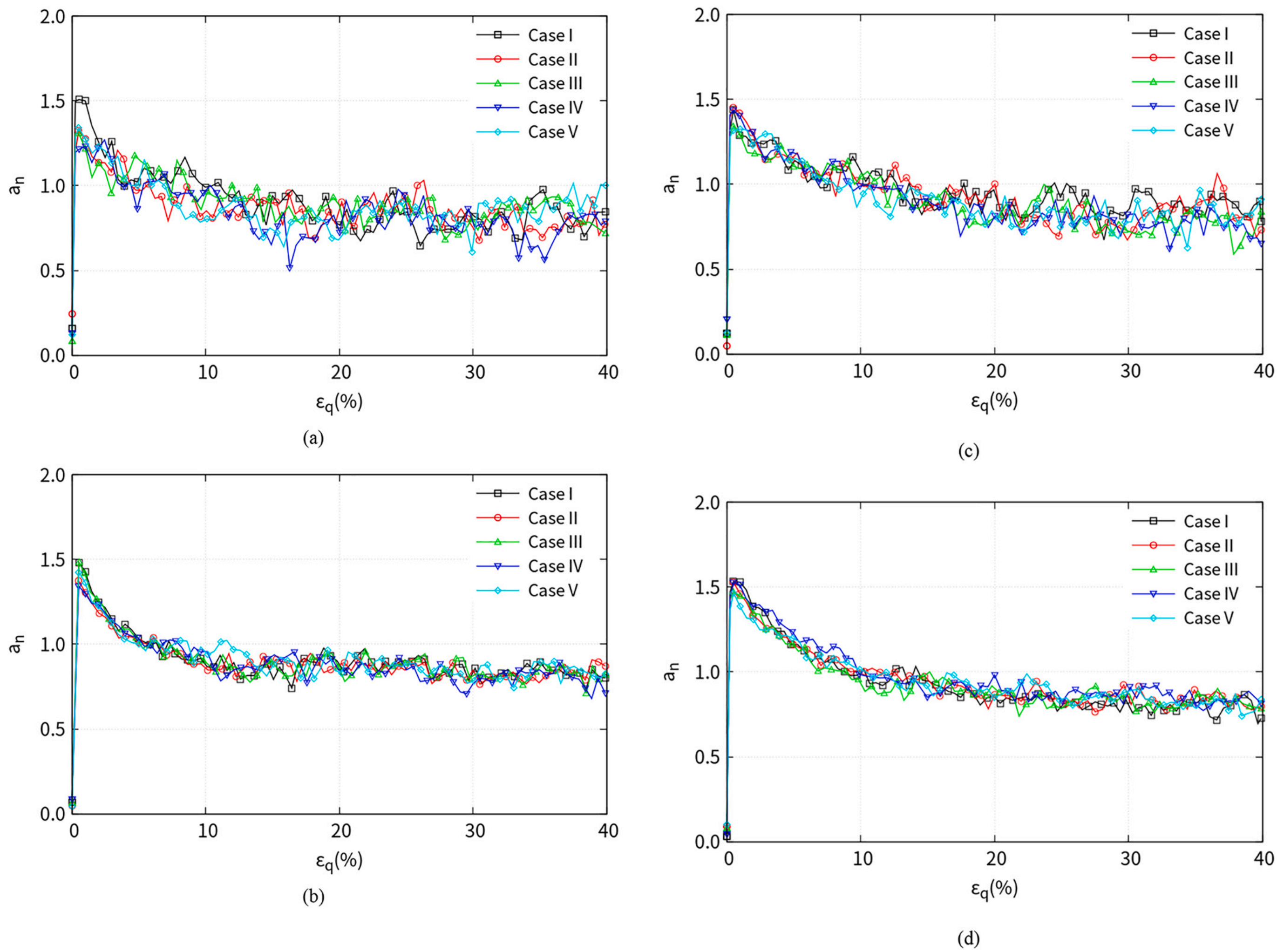

Fig. 9. Reproducibility of the normal force anisotropy: (a) $L/d_{max} = 6$ of PSD-I, (b) $L/d_{max} = 9$ of PSD-I, (c) $L/d_{max} = 8$ of PSD-II, (d) $L/d_{max} = 11$ of PSD-II.

Table 2
RVE sizes of different particle size distributions.

Coarse fraction	Particle size ratio					
	1	2	3	4.45	6	8
00%	13					
15%		7	6	4	4	3
30%		8	6	5	4	3
45%		9	7	5	5	4
60%		10	7	7	5	5
75%		12	11	9	8	7
90%		13	12	10	10	8
100%	13					

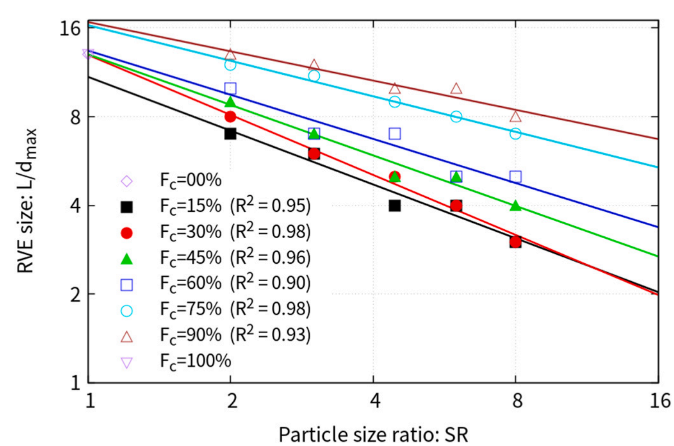

Fig. 10. Evolution diagram of the thresholds (L/d_{max}) for specimens with different particle size ratios ($D_r = 80\%$).

effect of the amorphous shape.

The mechanism of size effect may also be explained by the robustness of the skeleton. When the sample size is smaller than the RVE size, the structure is more variable due to the joint effect of sparsely distributed force chains and inter-grain slips [2,4,12,19]. As a result, the mechanical responses of these samples may show a noticeable fluctuation and poor reproducibility. In contrast, once the sample size reaches the RVE size, there is an adequate heterogeneity and the force chains disperse in the system to construct a percolating skeleton, which can be explained by the partial contacts between coarse grains and bridge effect of fine grains in gap-graded granular materials [27,48]. Consequently, sufficient heterogeneity and robustness of the structure help to reduce the scale-dependency and ensure the representativeness of mechanical properties. The size effect typically arises from variations in the microstructure of assemblies. It is of a great importance to explicitly reveal the origin at the micro-scale. This mechanism may be further investigated through complex network analysis and percolation theory in the future [33].

Table 3
Fitting parameters of empirical formulas. The R^2 is the coefficient of determination.

Coarse fraction	m	n	R^2
15%	10.92	−0.61	0.95
30%	12.97	−0.68	0.98
45%	13.02	−0.57	0.96
60%	13.41	−0.50	0.90
75%	16.35	−0.40	0.98
90%	16.76	−0.33	0.93

Table 4
Fitting formulas of coefficients and coarse fractions. The R^2 is the coefficient of determination.

Coefficient	Formula	R^2
m	$m = 0.0728F_c + 10.135$	0.90
n	$n = 0.0047F_c$ - 0.7666	0.93

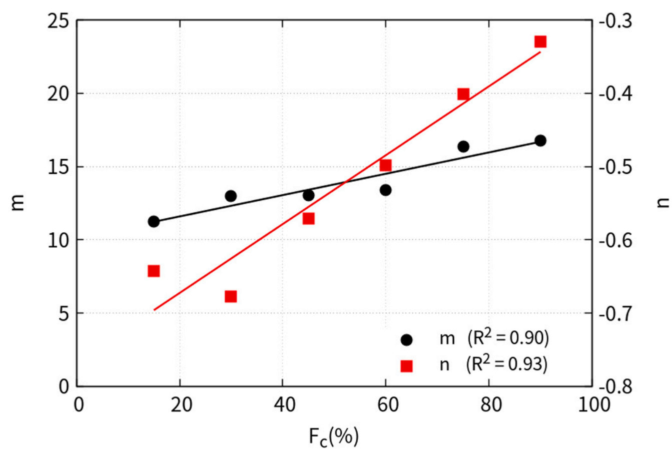

Fig. 11. Fitting coefficients versus coarse fractions.

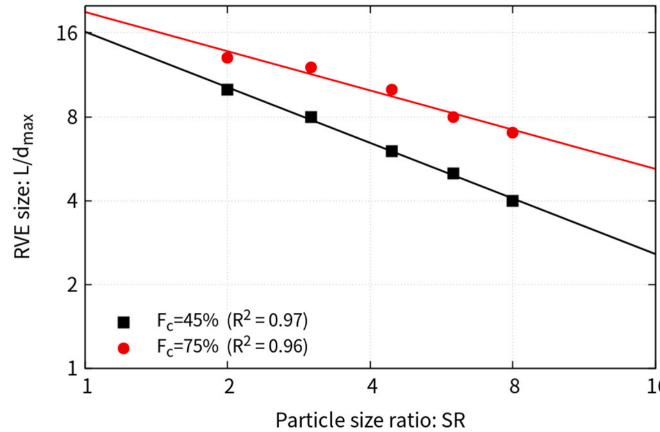

Fig. 12. Evolution diagram of the thresholds ($L/d_{\max}$) for specimens with different particle size ratios (D_r = 50%).

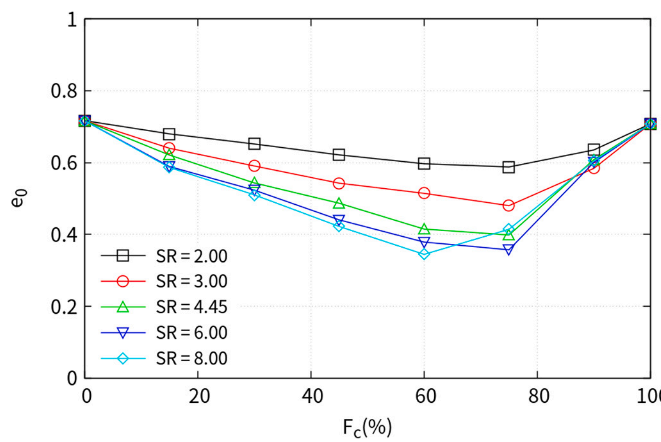

Fig. 13. The initial void ratios of RVE samples with various coarse fractions.

5. Conclusion

In this study, DEM simulations have been performed to investigate the size effect of gap-graded granular mixtures. The Chi-square test on three mechanical parameters is conducted to select the optimal RVE size. Furthermore, the responses of microscopic parameters are compared to verify the reproducibility of the RVE sizes. The influence of coarse fraction and particle size ratio on the RVE size is systematically analyzed. The important findings are summarized as follows:

(1) Gap-graded granular materials have strong scale dependency in terms of strength and deformation properties. The scatter of simulated mechanical properties decreases significantly with increasing sample size. All properties converge to their own asymptotic values when the sample size ratio reaches a threshold.
(2) The Chi-square criterion is introduced to statistically determine the RVE size for gap-graded granular mixtures. The variability of mechanical properties is negligible when the sample size is beyond the RVE size domain. Based on the statistical analysis, a total of 32 values of RVE size are determined for each particle size distribution and summarized in Table 2.
(3) Microstructural behaviors are analyzed to validate the determined RVE sizes. The microscopic responses of the samples with RVE sizes are more reproducible compared with those of small-scale samples, which indicates that the corresponding samples contain sufficient information on the microstructure to be statistically representative.
(4) The RVE size of gap-graded granular materials is affected by both coarse fraction and particle size ratio. RVE size increases with rising coarse fractions but falls as particle size ratios rise. Empirical equations are proposed to correlate RVE sizes with particle size ratio for various coarse fractions and confirmed for different relative densities.

CRediT authorship contribution statement

Xiusong Shi: Writing – original draft, Supervision, Methodology, Funding acquisition, Conceptualization. **Zihao He:** Writing – original draft, Software, Investigation, Formal analysis. **Jidong Zhao:** Writing – review & editing, Validation, Supervision. **Jiaying Liu:** Writing – review & editing, Supervision, Funding acquisition.

Declaration of competing interest

The authors declare that they have no known competing financial interests or personal relationships that could have appeared to influence the work reported in this paper.

Data availability

Data will be made available on request.

Acknowledgement

This study was partially supported by the National Natural Science Foundation of China (under Grant no. 52278346; Grant no. 12272334), the Research Grants Council of Hong Kong (under RGC/GRF Grant no. 16201419), and the Funds for the Disciplinary Development (Research Starting Funds for High-level Talents: Grant no. 522020212).

Appendix A

For the mechanical parameters used to determine the RVE size, the value of them of each realization X_n is assumed to be a stochastic value, following the normal distribution, which is compared with the average value $\overline{X}$ of each sample size ratio. The null hypothesis (H_0) is given

$$H_0 : X_n = \overline{X} \text{ for all realizations} \tag{15}$$

and the alternative hypothesis (H_A) would state.

$$H_\mathrm{A} : X_n \neq \overline{X} \text{ for at least one realization} \tag{16}$$

The Chi-square value is then calculated using the Eq. (13).

The accuracy of 95% is prescribed and the degree of freedom (k) is equal to 2, which results in the critical Chi-square value 0.103 in the distribution table. Note that the value of k is associated with the number of realizations (n) and the number of distribution parameters (m) which is 2 in the normal distribution containing mathematical expectation and standard deviation

$$k = n - m - 1 \tag{17}$$

The computed Chi-square values are compared with the critical value to decide whether to accept the null hypothesis or not. The null hypothesis is accepted if the Chi-square value is lower than 0.103, which indicates that the data satisfy the desired accuracy.

Appendix B

Macroscopic properties of Samples PSD-1 and PSD-2 (PSD shown in Fig. 4(c)) are shown in Fig. B.1-Fig. B.4. In these figures, similar trends of the peak friction angle, the dilatancy angle, etc., can be found as PSD-I and PSD-II

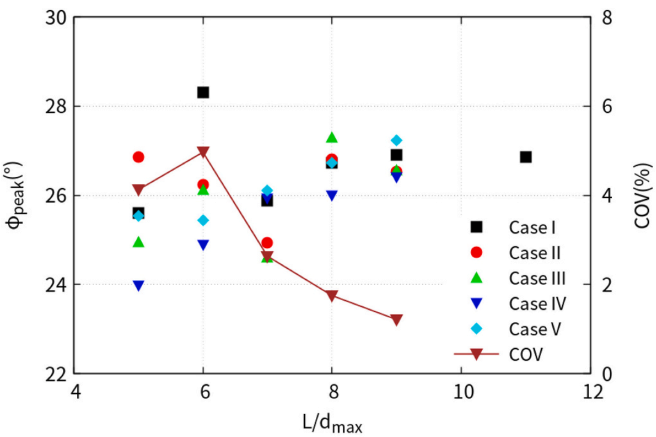

(a)

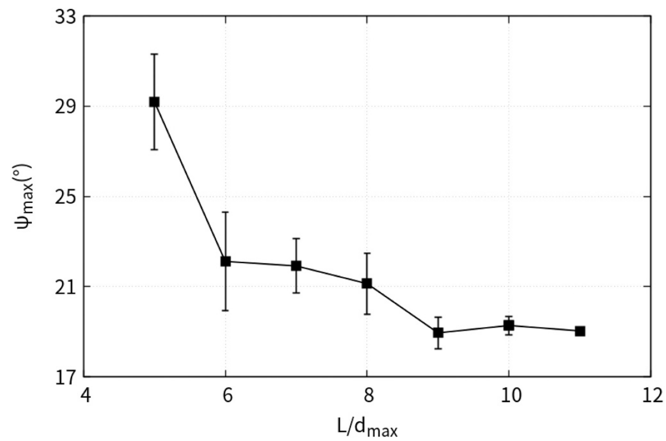

(d)

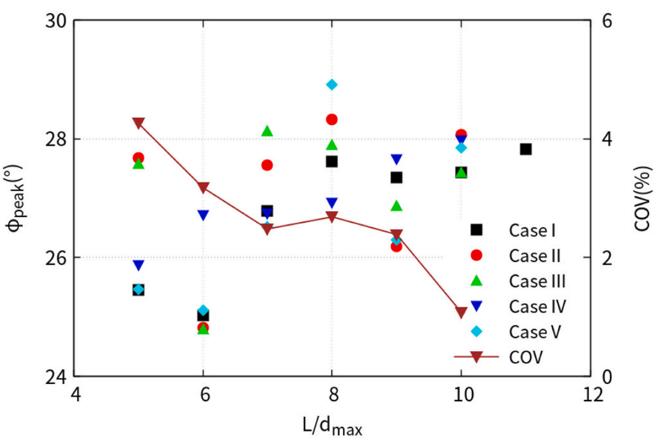

(b)

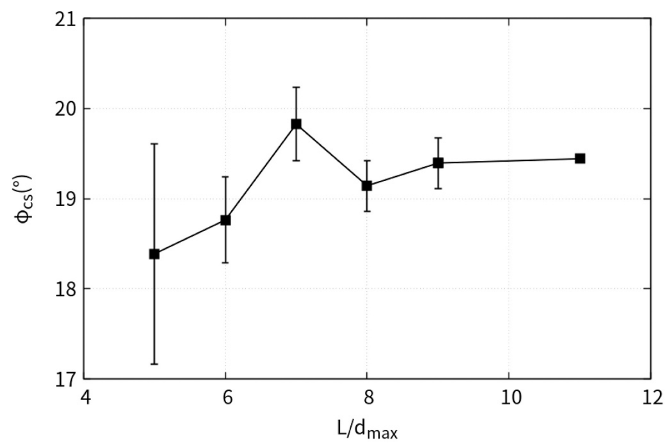

(e)

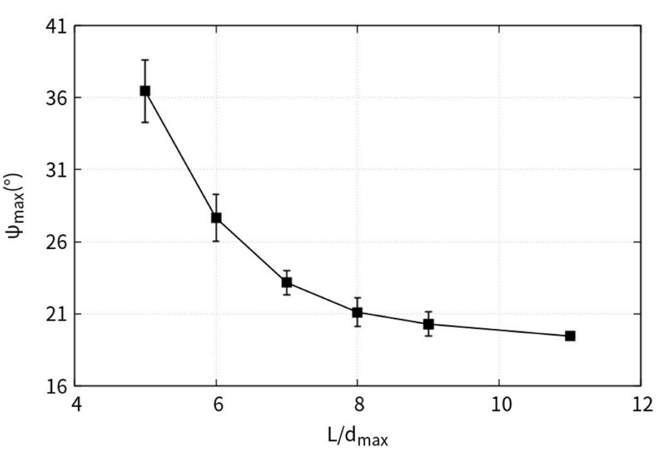

(c)

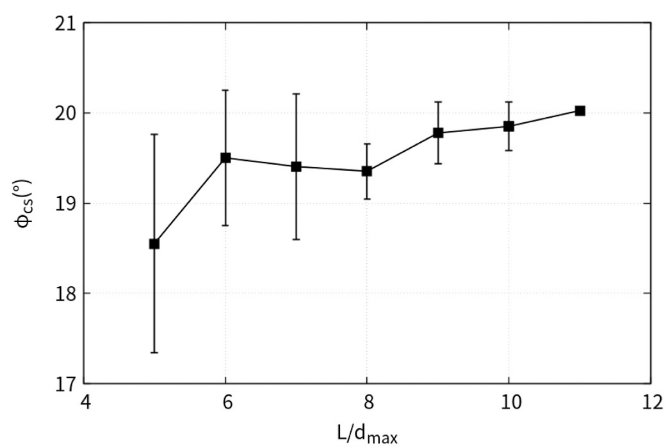

(f)

Fig. B.1. Results of simulated macroscopic properties: (a)-(b) peak friction angle and its coefficient of variation for PSD-1 and PSD-2, (c)-(d) average value and standard deviation of maximum dilatancy angle for PSD-1 and PSD-2, (e)-(f) average value and standard deviation of critical state friction angle for PSD-1 and PSD-2.

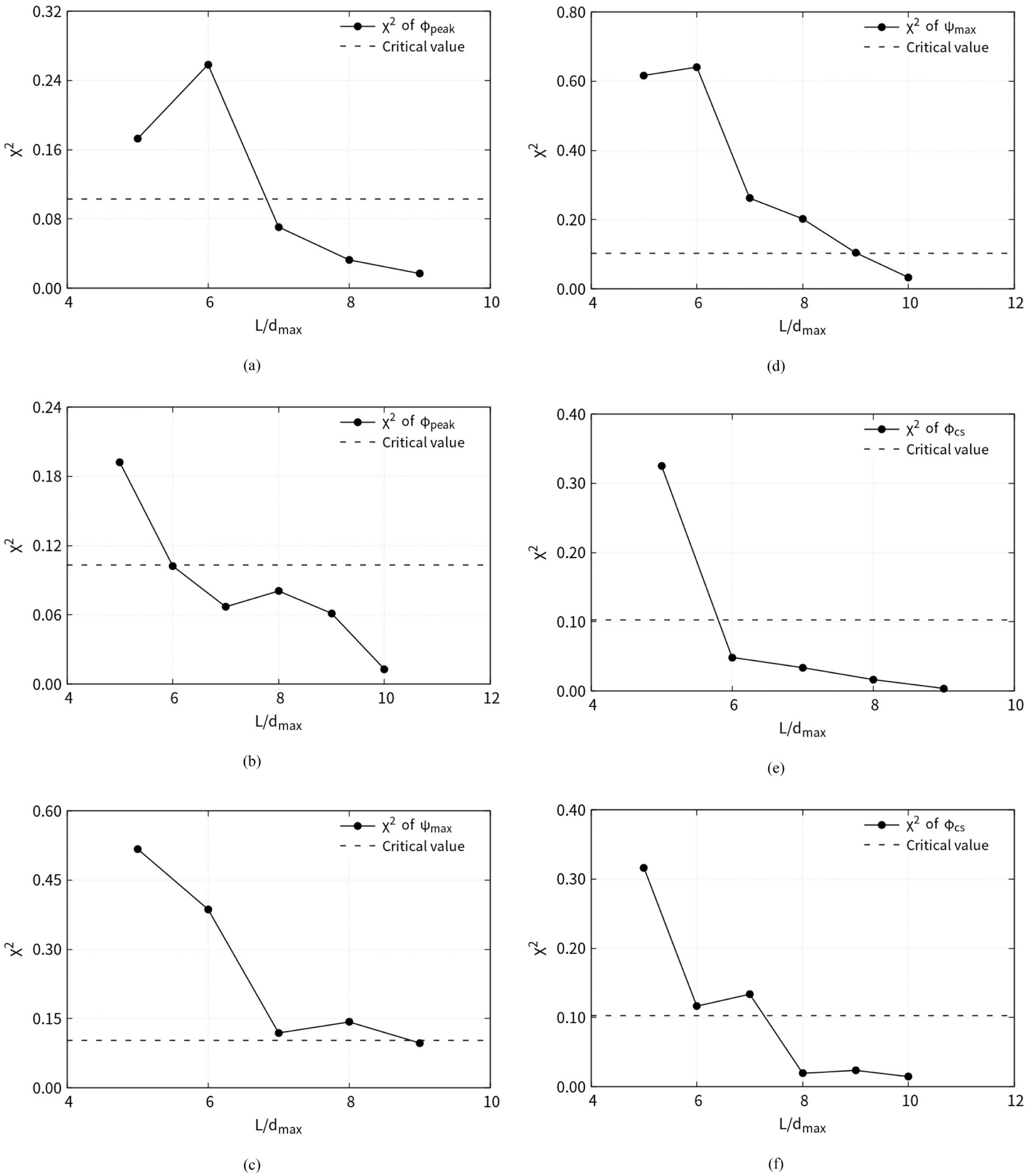

Fig. B.2. Chi-square values of macroscopic properties: (a)-(b) Chi-square values of peak friction angle for PSD-1 and PSD-2, (c)-(d) Chi-square values of maximum dilatancy angle for PSD-1 and PSD-2, (e)-(f) Chi-square values of critical state friction angle for PSD-1 and PSD-2.

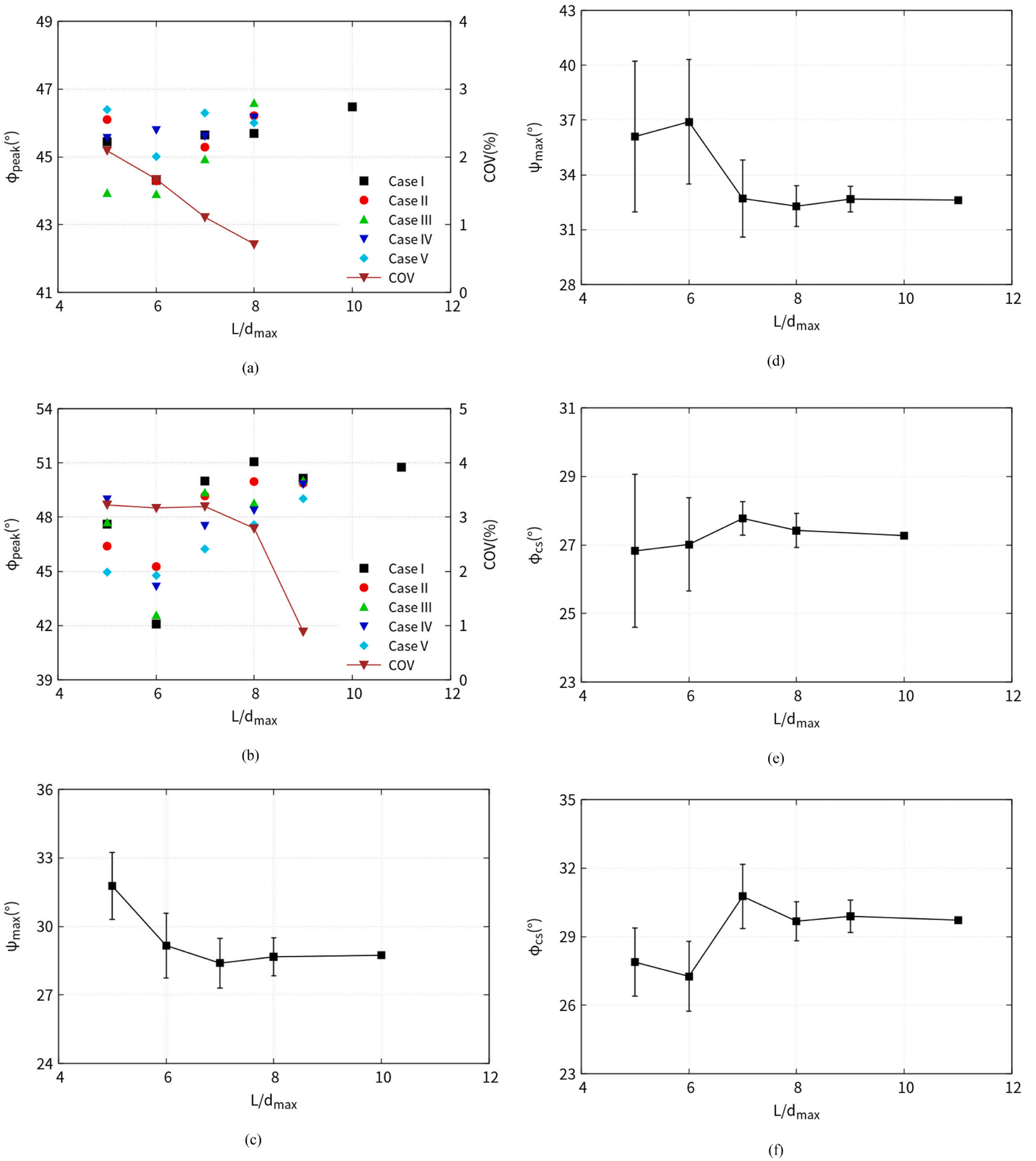

Fig. B.3. Results of simulated macroscopic properties of binary ellipsoid mixtures: (a)-(b) peak friction angle and its coefficient of variation for PSD-1 and PSD-2, (c)-(d) average value and standard deviation of maximum dilatancy angle for PSD-1 and PSD-2, (e)-(f) average value and standard deviation of critical state friction angle for PSD-1 and PSD-2.

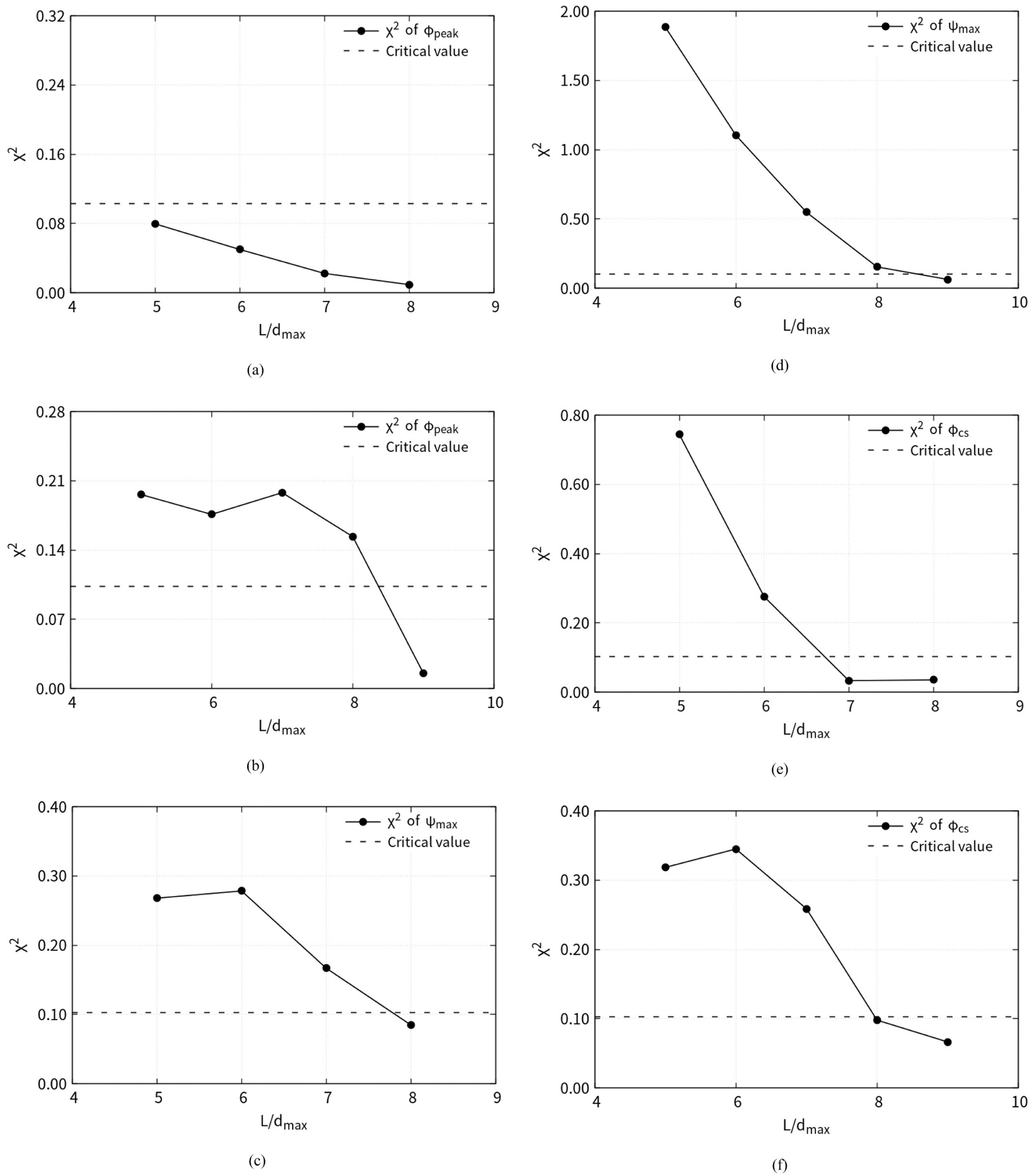

Fig. B.4. Chi-square values of macroscopic properties of binary ellipsoid mixtures: (a)-(b) Chi-square values of peak friction angle for PSD-1 and PSD-2, (c)-(d) Chi-square values of maximum dilatancy angle for PSD-1 and PSD-2, (e)-(f) Chi-square values of critical state friction angle for PSD-1 and PSD-2.

References

[1] P. Adesina, C. O'Sullivan, T. Morimoto, M. Otsubo, Determining a representative element volume for DEM simulations of samples with non-circular particles, Particuology 68 (2022) 29–43.

[2] K. Alshibli, L. Roussel, Experimental investigation of slip-stick behaviour in granular materials, Int. J. Numer. Anal. Methods Geomech. 30 (14) (2006) 1391–1407.

[3] R. Al-Raoush, A. Papadopoulos, Representative elementary volume analysis of porous media using X-ray computed tomography, Powder Technol. 200 (1–2) (2010) 69–77.

[4] N. An, G. Ma, H. Zhou, D. Wang, X. Lu, W. Zhou, DEM investigation of the microscopic mechanism of scale effect of sandy gravel material, Acta Geotech. (2022) 1–18.
[5] A.S.T.M. Standard, D7181., Standard Test Method for Consolidated Drained Triaxial Compression Test for Soils, ASTM International, West Conshohocken, PA, 2020.
[6] R.J. Bathurst, L. Rothenburg, Observations on stress-force-fabric relationships in idealized granular materials, Mech. Mater. 9 (1) (1990) 65–80.
[7] M. Bouchedjra, T. Kanit, C. Boulemia, A. Amrouche, M.E.A. Belouchrani, Determination of the RVE size for polycrystal metals to predict monotonic and cyclic elastoplastic behavior: statistical and numerical approach with new criteria, Eur. J. Mech. A/Solids 72 (2018) 1–15.
[8] B.S. Standard, 1377., British Standard Methods of Test for Soils for Civil Engineering Purposes, British Standards Institution, 1990.
[9] M.S. Costanza-Robinson, B.D. Estabrook, D.F. Fouhey, Representative elementary volume estimation for porosity, moisture saturation, and air-water interfacial areas in unsaturated porous media: data quality implications, Water Resour. Res. 47 (7) (2011) W07513.
[10] P.A. Cundall, O.D. Strack, A discrete numerical model for granular assemblies, Geotechnique 29 (1) (1979) 47–65.
[11] X. Ding, L. Zhang, H. Zhu, Q. Zhang, Effect of model scale and particle size distribution on PFC3D simulation results, Rock Mech. Rock. Eng. 47 (6) (2014) 2139–2156.
[12] P. Evesque, F. Adjemian, Stress fluctuations and macroscopic stick-slip in granular materials, Eur. Phys. J. E 9 (2002) 253–259.
[13] K. Esmaieli, J. Hadjigeorgiou, M. Grenon, Estimating geometrical and mechanical REV based on synthetic rock mass models at Brunswick Mine, Int. J. Rock Mech. Min. Sci. 47 (6) (2010) 915–926.
[14] K. Farahmand, I. Vazaios, M.S. Diederichs, N. Vlachopoulos, Investigating the scale-dependency of the geometrical and mechanical properties of a moderately jointed rock using a synthetic rock mass (SRM) approach, Comput. Geotech. 95 (2018) 162–179.
[15] I.M. Gitman, M.B. Gitman, H. Askes, Quantification of stochastically stable representative volumes for random heterogeneous materials, Arch. Appl. Mech. 75 (2006) 79–92.
[16] I.M. Gitman, H. Askes, L.J. Sluys, Representative volume: existence and size determination, Eng. Fract. Mech. 74 (16) (2007) 2518–2534.
[17] M. Goudarzy, D. König, T. Schanz, Small strain stiffness of granular materials containing fines, Soils Found. 56 (5) (2016) 756–764.
[18] S. Graham, N. Yang, Representative volumes of materials based on microstructural statistics, Scr. Mater. 48 (3) (2003) 269–274.
[19] N. Guo, J. Zhao, The signature of shear-induced anisotropy in granular media, Comput. Geotech. 47 (2013) 1–15.
[20] N. Guo, J. Zhao, Multiscale insights into classical geomechanics problems, Int. J. Numer. Anal. Methods Geomech. 40 (3) (2016) 367–390.
[21] N. Guo, J. Zhao, 3D multiscale modeling of strain localization in granular media, Comput. Geotech. 80 (2016) 360–372.
[22] W.M. Harris, W.K. Chiu, Determining the representative volume element size for three-dimensional microstructural material characterization. Part 1: Predictive models, J. Power Sources 282 (2015) 552–561.
[23] Z. Hashin, Analysis of composite materials—a survey, J. Appl. Mech. 50 (1983) 481–505.
[24] X. Huang, K.J. Hanley, C. O'Sullivan, F.C. Kwok, Effect of sample size on the response of DEM samples with a realistic grading, Particuology 15 (2014) 107–115.
[25] J.A. Hudson, J.P. Harrison, Engineering Rock Mechanics, Elsevier, Oxford, 1997.
[26] I. Ioannis, H. Alma, G. Inna, S. Costas, M.A. Almaadeed, Micro-mechanical parameters in short fibre composite, Appl. Compos. Mater. 21 (2014) 197–211.
[27] M.K. Jafari, A. Shafiee, Mechanical behavior of compacted composite clays, Can. Geotech. J. 41 (6) (2004) 1152–1167.
[28] T. Kanit, S. Forest, I. Galliet, V. Mounoury, D. Jeulin, Determination of the size of the representative volume element for random composites: statistical and numerical approach, Int. J. Solids Struct. 40 (13–14) (2003) 3647–3679.
[29] S.P.K. Kodicherla, G. Gong, L. Fan, S. Wilkinson, C.K. Moy, Investigations of the effects of particle morphology on granular material behaviors using a multi-sphere approach, J. Rock Mech. Geotech. Eng. 12 (6) (2020) 1301–1312.
[30] T. Koyama, L. Jing, Effects of model scale and particle size on micro-mechanical properties and failure processes of rocks—a particle mechanics approach, Eng. Anal. Bound. Elem. 31 (5) (2007) 458–472.
[31] M.R. Kuhn, K. Bagi, Specimen size effect in discrete element simulations of granular assemblies, J. Eng. Mech. 135 (6) (2009) 485–492.
[32] A.K.H. Kwan, K.W. Chan, V. Wong, A 3-parameter particle packing model incorporating the wedging effect, Powder Technol. 237 (2013) 172–179.
[33] J. Liu, X. Wu, J. Jiang, Z. Ding, C. Lü, X. Shi, A network-based investigation on the strong contact system of granular materials under isotropic and deviatoric stress states, Comput. Geotech. 153 (2023) 105077.
[34] Z. Liu, C. Zhang, C. Zhang, H. Wang, H. Zhou, B. Zhou, Effects of amygdale heterogeneity and sample size on the mechanical properties of basalt, J. Rock Mech. Geotech. Eng. 14 (1) (2022) 93–107.
[35] R.D. Mindlin, H. Deresiewicz, Elastic Spheres in Contact under Varying Oblique Forces, 1953.
[36] T.T. Ng, Input parameters of discrete element methods, J. Eng. Mech. 132 (7) (2006) 723–729.
[37] T.T. Ng, W. Zhou, Sample size effect on DEM simulations of binary mixture, in: International Conference on Discrete Element Methods, 2016, pp. 73–80.
[38] T.T. Ng, W. Zhou, G. Ma, X.L. Chang, Macroscopic and microscopic behaviors of binary mixtures of different particle shapes and particle sizes, Int. J. Solids Struct. 135 (2018) 74–84.
[39] T.K. Nguyen, On the representative volume element of dense granular assemblies made of 2D circular particles, in: Structural Health Monitoring and Engineering Structures, 2021, pp. 499–508.
[40] T. Omar, A. Sadrekarimi, Specimen size effects on behavior of loose sand in triaxial compression tests, Can. Geotech. J. 52 (6) (2015) 732–746.
[41] M. Ostoja-Starzewski, Microstructural randomness versus representative volume element in thermomechanics, J. Appl. Mech. 69 (1) (2002) 25–35.
[42] C. O'Sullivan, Particulate Discrete Element Modelling: A Geomechanics Perspective, CRC Press, 2011.
[43] C. Pélissou, J. Baccou, Y. Monerie, F. Perales, Determination of the size of the representative volume element for random quasi-brittle composites, Int. J. Solids Struct. 46 (14–15) (2009) 2842–2855.
[44] J.P. Plassiard, N. Belheine, F.V. Donzé, A spherical discrete element model: calibration procedure and incremental response, Granul. Matter 11 (5) (2009) 293–306.
[45] L. Rothenburg, N.P. Kruyt, Critical state and evolution of coordination number in simulated granular materials, Int. J. Solids Struct. 41 (21) (2004) 5763–5774.
[46] S. Schmidt, M. Wiebicke, I. Herle, On the determination and evolution of fabric in representative elementary volumes for a sand specimen in triaxial compression, Granul. Matter 24 (4) (2022) 1–9.
[47] G. Shahin, E.B. Herbold, S.A. Hall, R.C. Hurley, Quantifying the hierarchy of structural and mechanical length scales in granular systems, Extreme Mech. Lett. 51 (2022) 101590.
[48] X. Shi, K. Liu, J. Yin, Effect of initial density, particle shape, and confining stress on the critical state behavior of weathered gap-graded granular soils, J. Geotech. Geoenviron. Eng. 147 (2) (2021) 04020160.
[49] X. Shi, J. Nie, J. Zhao, Y. Gao, A homogenization equation for the small strain stiffness of gap-graded granular materials, Comput. Geotech. 121 (2020) 103440.
[50] X. Shi, J. Zhao, Y. Gao, A homogenization-based state-dependent model for gap-graded granular materials with fine-dominated structure, Int. J. Numer. Anal. Methods Geomech. 45 (8) (2021) 1007–1028.
[51] V. Šmilauer, B. Chareyre, Yade DEM Formulation[M], Yade Documentation, 2011.
[52] M. Stroeven, H. Askes, L. Sluys, Numerical determination of representative volumes for granular materials, Comput. Methods Appl. Mech. Eng. 193 (30−32) (2004) 3221–3238.
[53] T. Wang, A. Wautier, S. Liu, F. Nicot, How fines content affects granular plasticity of under-filled binary mixtures, Acta Geotech. 17 (6) (2022) 2449–2463.
[54] H.Z. Wei, W.J. Xu, X.F. Xu, Q.S. Meng, C.F. Wei, Mechanical properties of strongly weathered rock–soil mixtures with different rock block contents, Int. J. Geomech. 18 (5) (2018) 04018026.
[55] J. Wiącek, M. Molenda, Effect of particle size distribution on micro-and macromechanical response of granular packings under compression, Int. J. Solids Struct. 51 (25–26) (2014) 4189–4195.
[56] J. Wiącek, M. Molenda, Representative elementary volume analysis of polydisperse granular packings using discrete element method, Particuology 27 (2016) 88–94.
[57] X. Xu, S. Wu, Y. Gao, M. Xu, Effects of micro-structure and micro-parameters on Brazilian tensile strength using flat-joint model, Rock Mech. Rock. Eng. 49 (9) (2016) 3575–3595.
[58] J. Xu, J. Liu, X. Shi, F. Ji, Y. Zeng, DEM investigation of the effect of coarse content and size ratio on the local shear behavior at gap-graded soil-structure interface, Powder Technol. 433 (2024) 119281.
[59] S. Yang, J. Dirrenberger, E. Monteiro, N. Ranc, Representative volume element size determination for viscoplastic properties in polycrystalline materials, Int. J. Solids Struct. 158 (2019) 210–219.
[60] Y. Yilmaz, Y. Deng, C.S. Chang, A. Gokce, Strength–dilatancy and critical state behaviours of binary mixtures of graded sands influenced by particle size ratio and fines content, Géotechnique (2021) 1–16.
[61] S. Zhang, H. Tang, H. Zhan, G. Lei, H. Cheng, Investigation of scale effect of numerical unconfined compression strengths of virtual colluvial–deluvial soil–rock mixture, Int. J. Rock Mech. Min. Sci. 77 (2015) 208–219.
[62] W. Zhang, J. Chen, H. Chen, D. Xu, Y. Li, Determination of RVE with consideration of the spatial effect, Int. J. Rock Mech. Min. Sci. 61 (2013) 154–160.
[63] J. Zhao, N. Guo, Unique critical state characteristics in granular media considering fabric anisotropy, Géotechnique 63 (8) (2013) 695–704.
[64] J. Zhao, N. Guo, The interplay between anisotropy and strain localisation in granular soils: a multiscale insight, Géotechnique 65 (8) (2015) 642–656.
[65] S. Zhao, X. Zhou, Effects of particle asphericity on the macro-and micro-mechanical behaviors of granular assemblies, Granul. Matter 19 (2017) 1–18.
[66] S. Zhao, T.M. Evans, X. Zhou, Three-dimensional Voronoi analysis of monodisperse ellipsoids during triaxial shear, Powder Technol. 323 (2018) 323–336.
[67] C. Zhou, K. Li, F. Ma, Numerical and statistical analysis of elastic modulus of concrete as a three-phase heterogeneous composite, Comput. Struct. 139 (2014) 33–42.

[68] W. Zhou, J. Liu, G. Ma, W. Yuan, X. Chang, Macroscopic and microscopic behaviors of granular materials under proportional strain path: a DEM study, Int. J. Numer. Anal. Methods Geomech. 40 (18) (2016) 2450–2467.
[69] W. Zhou, K. Xu, G. Ma, L. Yang, X. Chang, Effects of particle size ratio on the macro-and microscopic behaviors of binary mixtures at the maximum packing efficiency state, Granul. Matter 18 (4) (2016) 1–13.
[70] W. Zhou, J. Liu, G. Ma, X. Chang, Three-dimensional DEM investigation of critical state and dilatancy behaviors of granular materials, Acta Geotech. 12 (2017) 527–540.
[71] Y. Zhu, J. Gong, Z. Nie, Numerical investigation of the elastic properties of binary mixtures as a function of the size ratio and fines content[J], Int. J. Geomech. 20 (9) (2020) 04020155.
[72] Y. Zhu, Z. Nie, J. Gong, J. Zou, L. Zhao, L. Li, An analysis of the effects of the size ratio and fines content on the shear behaviors of binary mixtures using DEM, Comput. Geotech. 118 (2020) 103353.
[73] L. Zuo, B.A. Baudet, Determination of the transitional fines content of sand-non plastic fines mixtures, Soils Found. 55 (1) (2015) 213–219.